Fractional-Calculus-Based FDTD Algorithm for Ultrawideband Electromagnetic Characterization of Arbitrary Dispersive Dielectric Materials

Fractional–Calculus–Based FDTD Algorithm for Ultrawideband Electromagnetic Characterization of Arbitrary Dispersive Dielectric Materials

Diego Caratelli, *Member, IEEE*, Luciano Mescia, Pietro Bia, *Student Member, IEEE*, and Oleg V. Stukach, *Member, IEEE*

***Abstract*—A novel finite–difference time–domain algorithm for modeling ultra–wideband electromagnetic pulse propagation in arbitrary multi–relaxed dispersive media is presented. The proposed scheme is based on a general, yet computationally efficient, series representation of the fractional derivative operators associated with the permittivity functions describing the frequency dispersion properties of a given dielectric material. Dedicated uniaxial perfectly matched layer boundary conditions are derived and implemented in combination with the basic time–marching scheme. Moreover, a total field/scattered field formulation is adopted in order to analyze the material response under plane–wave excitation. Compared to alternative numerical methodologies available in the scientific literature, the proposed technique features a significantly enhanced robustness and accuracy which are essential for solving complex electromagnetic propagation problems.**

***Index Terms*—Dispersive Media, Finite–Difference Time–Domain, Fractional Calculus, Dielectric Relaxation.**

I. Introduction

THE modeling of electromagnetic field propagation in disordered dielectrics, such as polymers, biopolymers, biomolecules, biological tissues, colloids, and porous materials, is a subject of increasing importance for a growing number of engineering applications [1]–[3]. As a matter of fact, the development of theoretical models and computational techniques for the analysis of the interaction between pulsed electric fields (*PEFs*) and disordered dielectrics is instrumental for gaining a deeper insight into the involved physical mechanisms. Said materials exhibit, both at microscopic and macroscopic scale, complex relaxation dynamics which cannot be described by a conventional exponential law. In order to overcome this limitation and provide an enhanced description of non–exponential dielectric relaxation processes, a number of empirical dispersion functions, such as Cole–Cole, Cole–Davidson, Havriliak–Negami, Jonscher, and Raicu, have been introduced in the scientific literature [4].

The finite–difference time–domain (*FDTD*) method has been widely used in electromagnetic analysis due to its straightforward implementation and ability to model a broad range of exposure conditions [5], [6]. Since the aforementioned dispersion functions include fractional powers of the angular frequency ω, suitable mathematical models, adequately describing the response of such complex dispersive materials, have to be embedded in the core of the *FDTD* algorithm [7]–[9]. To that end, a novel methodology has been recently introduced by the authors in [1] in order to characterize Havriliak–Negami (*HN*) materials with single relaxation time τ, and general dispersion parameters α, β. Such formulation is based on the optimal truncation of the binomial series relevant to the *HN* fractional derivative operator, in accordance with the Riemann–Liouville theory. By performing several test cases, it has been found out that, for $\omega\tau \lesssim 10$, $\alpha < 0.5$, and $\beta < 0.25$, the mentioned approach provides a reliable and very accurate approximation of both the real and imaginary parts of *HN* permittivity functions over broad frequency ranges [1]. On the other hand, further investigations have highlighted that, for $\alpha > 0.5$ and $\beta > 0.25$, numerical inaccuracies can possibly occur wherein the truncated series expansion is used to model the *HN* material behavior over ultra–wide bands ($\omega\tau \geqslant 10$) [10]. In order to overcome these limitations, the authors have extended the previously presented *FDTD* scheme by implementing a more general series representation of the fractional derivative operators that, furthermore, allows accounting for multiple higher–order dispersive relaxation processes and ohmic losses. The enhanced accuracy of the modified *FDTD* procedure has been assessed by several test cases involving complex dielectric media, and compared against a fully analytical modeling approach.

The paper is organized as follows. In Section II the extended fractional–calculus–based model for dielectric dispersion is proposed, and the associated *FDTD* algorithm is derived while devoting emphasis to the relevant numerical stability and derivation of dedicated absorbing boundary conditions. Numerical results illustrating the soundness of the proposed methodology are then presented in Section III. The concluding remarks are summarized in Section IV.

II. Mathematical Formulation

The macroscopic dielectric properties of materials with disordered structure are determined by the interaction of the electromagnetic energy with the material constituents at microscopic and mesoscopic scale, as well as by the intermolecular

Manuscript received on January 16, 2016.

D. Caratelli is with The Antenna Company Nederland B.V., High Tech Campus, Eindhoven, The Netherlands, and the Institute of Cybernetics, Tomsk Polytechnic University, 84/3 Sovetskaya Street – 634050, Tomsk, Russia. e-mail: diego.caratelli@antennacompany.com.

L. Mescia and P. Bia are with the Department of Electrical and Information Engineering, Politecnico di Bari, via E. Orabona 4 – 70125, Bari, Italy. e-mail: luciano.mescia@poliba.it, pietro.bia@poliba.it.

O. Stukach is with the Institute of Cybernetics, Tomsk Polytechnic University, 84/3 Sovetskaya Street – 634050, Tomsk, Russia. e-mail: os2@tpu.ru.

and dipole–dipole interactions. As a result, the permittivity and electrical conductivity vary from material to material and depend on the working frequency. In order to accurately model the electromagnetic wave propagation over broad frequency ranges, suitable analytical models of the dielectric properties are needed. In particular, the characteristics of a general dispersive medium exhibiting multi–relaxation processes can be modeled by using the following relationship:

$$\varepsilon_r(\omega) = \varepsilon_{r_\infty} + \sum_{l=1}^{N} \frac{\Delta\varepsilon_{r_l}}{\Gamma_l(j\omega\tau_l)} + \frac{\sigma}{j\omega\varepsilon_0}, \tag{1}$$

where $\omega = 2\pi f$ is the angular frequency, ε_{r_∞} denotes the asymptotic relative permittivity at high frequency (for $\omega \to +\infty$), $\Delta\varepsilon_{r_l}$ is a dimensional constant (also called the dielectric increment in some cases), and $\Gamma_l(j\omega\tau_l)$ is a heuristically derived fitting function depending on the characteristic time τ_l for $l = 1, 2, \ldots, N$, with N being the number of relaxation processes occurring in the considered dielectric material. In (1), as usual, σ is the static ionic conductivity, and ε_0 denotes the permittivity of free space. For consistency of the representation, we assume furthermore that the following condition holds true:

$$\lim_{\omega \to +\infty} |\Gamma_l(j\omega\tau_l)| = +\infty. \tag{2}$$

By using the expression (1), one can synthesize a wide variety of different dielectric dispersion laws, such as the classical ones [11]:

- Debye (*D*): $\Gamma(j\omega\tau) = 1 + j\omega\tau$,
- Cole–Cole (*CC*): $\Gamma(j\omega\tau) = 1 + (j\omega\tau)^{\alpha}$,
- Cole–Davidson (*CD*): $\Gamma(j\omega\tau) = (1 + j\omega\tau)^{\beta}$,
- Havriliak–Negami (*HN*): $\Gamma(j\omega\tau) = \left[1 + (j\omega\tau)^{\alpha}\right]^{\beta}$,
- Raicu (*R*): $\Gamma(j\omega\tau) = \left[(j\omega\tau)^{s} + (j\omega\tau)^{\alpha}\right]^{\beta}$,

with the parameters α, β, and s determining shape and behavioral features of the permittivity function. Clearly, more complex laws resulting from the generalization or combination of those listed above can be handled similarly.

A. Fractional–Calculus–Based Dielectric Dispersion Model

In the proposed *FDTD* scheme, the following approximated fractional expansion is adopted in place of the truncated binomial series representation introduced in [1]:

$$\Gamma_l(j\omega\tau_l) \simeq \sum_{n=0}^{K_l} \chi_{n,l} (j\omega\tau_l)^{\zeta_{n,l}} = \Gamma_l^{(a)}\left(j\omega\tau_l, \zeta_{n,l}, \chi_{n,l}\right), \tag{3}$$

where $\zeta_{n,l}$ and $\chi_{n,l}$ denote suitable real-valued parameters.

Let $K_{\max}$ be the maximum expansion order in (3), and δ be a given small positive threshold to be used for controlling the accuracy of the approximation. In this way, the parameters K_l, $\zeta_{n,l}$, and $\chi_{n,l}$ can be evaluated, for $l = 1, 2, \ldots, N$, by means of the following algorithm:

1) Initialize $K_l = 1$, and set the working frequency range $\omega_{\min} \leqslant \omega \leqslant \omega_{\max}$;
2) Define the relative error function:

$$e_{r_l}(\tau_l, \zeta_{n,l}, \chi_{n,l}) = \\ = \sqrt{\frac{\int_{\omega_{\min}}^{\omega_{\max}} \left|\Gamma_l(j\omega\tau_l) - \Gamma_l^{(a)}\left(j\omega\tau_l, \zeta_{n,l}, \chi_{n,l}\right)\right|^2 d\omega}{\int_{\omega_{\min}}^{\omega_{\max}} \left|\Gamma_l(j\omega\tau_l)\right|^2 d\omega}}; \tag{4}$$

3) Determine $\chi_{n,l}$ and $\zeta_{n,l}$ corresponding to the minimum of $e_{r_l}(\tau_l, \zeta_{n,l}, \chi_{n,l})$;
4) If $e_{r_l} \leq \delta$ or $K_l = K_{\max}$ stop, otherwise update the expansion order as $K_l \to K_l + 1$, and go to step 2.

In particular, the minimization of the error function in (4) is here carried out by means of a dedicated numerical procedure based on the enhanced weighted quantum particle swarm optimization (*EWQPSO*) technique proposed in [12], by virtue of the superior effectiveness in terms of convergence rate and accuracy in comparison to alternative heuristic search methods available in the scientific literature [13], [14]. As a matter of fact, contrary to conventional evolutionary algorithms, the developed *EWQPSO* technique does not rely on complex operators or require gradient information, and is therefore characterized by reduced computational time, and low memory usage [15].

B. Basic Time–Marching Scheme

The evaluation of the electromagnetic field distribution excited within the dielectric material under analysis is performed by using an extended formulation of the *FDTD* scheme proposed in [1], useful to model the ohmic losses as well as the multi–relaxation response of media with fractional–power–law frequency dispersion.

Let us consider a non–magnetic dispersive medium with complex relative permittivity described by (1). Under such assumption, the differential version of the Ampere's law in time domain, within said material, can be written as:

$$\nabla \times \mathbf{H} = \varepsilon_0 \varepsilon_{r_\infty} \partial_t \mathbf{E} + \sigma \mathbf{E} + \sum_{l=1}^{N} \mathbf{J}_l, \tag{5}$$

with ∂_t denoting the partial derivative operator with respect to time, and where the auxiliary displacement current density terms $\mathbf{J}_l$ ($l = 1, 2, \ldots, N$) have been introduced. It is straightforward to find out that the k–th term ($1 \leq k \leq N$) is such to satisfy the equation:

$$\mathscr{D}_t^{(k)} \mathbf{J}_k = \varepsilon_0 \Delta\varepsilon_{r_k} \partial_t \mathbf{E}, \tag{6}$$

involving the generalized fractional derivative operator:

$$\mathscr{D}_t^{(k)} = \mathscr{F}^{-1}\{\Gamma_k(j\omega\tau_k)\} \simeq \sum_{n=0}^{K_k} \chi_{n,k} \tau_k^{\zeta_{n,k}} \mathrm{D}_t^{\zeta_{n,k}}. \tag{7}$$

Upon substituting (6) in (5), and applying a second–order accurate finite–difference scheme, one readily obtains, at the time instant $t = m\Delta t$:

$$(\nabla \times \mathbf{H})|^m - \frac{\varepsilon_{r_\infty}}{\Delta\varepsilon_{r_k}} \left(\mathscr{D}_t^{(k)} \mathbf{J}_k\right)\Big|^m = \sum_{l=1}^{N} \mathbf{J}_l|^m + \sigma\, \mathbf{E}|^m, \tag{8}$$

where the vector terms appearing on the right–hand side of the equation are evaluated by means of the semi–implicit approximation:

$$\left\{ \begin{array}{c} \mathbf{J}_l \\ \mathbf{E} \end{array} \right\}\Big|^m = \frac{1}{2}\left(\left\{ \begin{array}{c} \mathbf{J}_l \\ \mathbf{E} \end{array} \right\}\Big|^{m-\frac{1}{2}} + \left\{ \begin{array}{c} \mathbf{J}_l \\ \mathbf{E} \end{array} \right\}\Big|^{m+\frac{1}{2}} \right). \tag{9}$$

In a similar way, from equation (6) it follows that:

$$\mathbf{E}|^{m+\frac{1}{2}} = \mathbf{E}|^{m-\frac{1}{2}} + \frac{\Delta t}{\varepsilon_0 \Delta \varepsilon_{r_k}} \left(\mathscr{D}_t^{(k)} \mathbf{J}_k \right)\Big|^m. \tag{10}$$

Let $\nu_{n,k}$ be the integer number such that $\nu_{n,k}-1 \leqslant \zeta_{n,k} \leqslant \nu_{n,k}$. So, applying the Riemann–Liouville theory based procedure detailed in [1] for the finite-difference approximation of the operator $\mathscr{D}_t^{(k)}$ yields, after some mathematical manipulations which are omitted here:

$$\left(\mathscr{D}_t^{(k)} \mathbf{J}_k \right)\Big|^m \simeq \sum_{n=0}^{K_k} \frac{\chi_{n,k}}{(\nu_{n,k}-\zeta_{n,k})!} \left(\frac{\tau_k}{\Delta t} \right)^{\zeta_{n,k}} \sum_{p=0}^{\nu_{n,k}} \left[A_{n,k,p}\, \mathbf{J}_k|^{m-p+\frac{1}{2}} + \sum_{q=1}^{Q_{n,k}} B_{n,k,p,q}\, \mathbf{\Psi}_{n,k,q}\Big|^{m-p} \right], \tag{11}$$

with:

$$\left\{ \begin{array}{c} A_{n,k,p} \\ B_{n,k,p,q} \end{array} \right\} = (-1)^p \binom{\nu_{n,k}}{p} \left\{ \begin{array}{c} \sum_{q=1}^{Q_{n,k}} a_{n,k,q} \\ e^{-b_{n,k,q}} \end{array} \right\}, \tag{12}$$

the coefficients $a_{n,k,q}$ and $b_{n,k,q}$ for $q = 1,2,\ldots,Q_{n,k}$ resulting from the non–linear least–square minimization of the function:

$$W_{n,k}(p) = \left| (p+1)^{\nu_{n,k}-\zeta_{n,k}} - p^{\nu_{n,k}-\zeta_{n,k}} - \sum_{q=1}^{Q_{n,k}} a_{n,k,q} e^{-b_{n,k,q}p} \right|, \tag{13}$$

depending on the integer index p. In (11), $\mathbf{\Psi}_{n,k,q}$ denotes the auxiliary current density vector defined by the following recursion formula:

$$\mathbf{\Psi}_{n,k,q}\Big|^m = \left\{ \begin{array}{ll} a_{n,k,q}\, \mathbf{J}_k|^{m-\frac{1}{2}} + e^{-b_{n,k,q}}\, \mathbf{\Psi}_{n,k,q}\Big|^{m-1}, & m \geqslant 1, \\ 0, & m \leqslant 0. \end{array} \right. \tag{14}$$

Finally, by combining (8) with (9), (10), (11), one can readily obtain:

$$\begin{aligned} &\left[\left(\varepsilon_{r_\infty} + \frac{\sigma \Delta t}{2\varepsilon_0} \right) \frac{C_k}{\Delta \varepsilon_{r_k}} + \frac{1}{2} \right] \mathbf{J}_k|^{m+\frac{1}{2}} + \frac{1}{2} \sum_{l=1, l\neq k}^{N} \mathbf{J}_l|^{m+\frac{1}{2}} = \\ &= (\nabla \times \mathbf{H})|^m - \sigma \mathbf{E}|^{m-\frac{1}{2}} - \frac{1}{2} \sum_{l=1}^{N} \mathbf{J}_l|^{m-\frac{1}{2}} - \left(\varepsilon_{r_\infty} + \frac{\sigma \Delta t}{2\varepsilon_0} \right) \\ &\cdot \frac{1}{\Delta \varepsilon_{r_k}} \sum_{n=0}^{K_k} \frac{\chi_{n,k}}{(\nu_{n,k}-\zeta_{n,k})!} \left(\frac{\tau_k}{\Delta t} \right)^{\zeta_{n,k}} \left[\sum_{p=1}^{\nu_{n,k}} A_{n,k,p}\, \mathbf{J}_k|^{m-p+\frac{1}{2}} \right. \\ &\left. + \sum_{p=0}^{\nu_{n,k}} \sum_{q=1}^{Q_{n,k}} B_{n,k,p,q}\, \mathbf{\Psi}_{n,k,q}\Big|^{m-p} \right] = \boldsymbol{\eta}_k|^m, \end{aligned} \tag{15}$$

where:

$$C_k = \sum_{n=0}^{K_k} A_{n,k,0} \frac{\chi_{n,k}}{\nu_{n,k}-\zeta_{n,k}} \left(\frac{\tau_k}{\Delta t} \right)^{\zeta_{n,k}}, \tag{16}$$

for $k = 1,2,\ldots,N$. It is apparent from (15) that in the presented formulation, contrary to the methodology in [1], the evaluation of the displacement current density entails solving a symmetric system of N linear equations, this reflecting the multi–relaxation characteristics of the dielectric material under analysis. As a matter of fact, equations (15) can be recast in the more compact matrix form:

$$\underbrace{\left[\frac{1}{2} \underline{\mathbf{U}} + \left(\varepsilon_{r_\infty} + \frac{\sigma \Delta t}{2\varepsilon_0} \right) \underline{\mathbf{D}} \right]}_{\underline{\mathbf{T}}} \cdot \mathbf{J}|^{m+\frac{1}{2}} = \boldsymbol{\eta}|^m, \tag{17}$$

with $\underline{\mathbf{U}}$ being the unit matrix of order N, and $\underline{\mathbf{D}} = \mathrm{diag}\{D_1, D_2, \ldots, D_N\}$ the diagonal matrix with nonzero entries $D_k = C_k/\Delta\varepsilon_{r_k}$. In (17), $\mathbf{J}|^{m+\frac{1}{2}}$ denotes the vector of the unknown current densities at the time instant $t = \left(m+\frac{1}{2}\right)\Delta t$, namely:

$$\mathbf{J}|^{m+\frac{1}{2}} = \left[\begin{array}{c} \mathbf{J}_1|^{m+\frac{1}{2}} \\ \mathbf{J}_2|^{m+\frac{1}{2}} \\ \vdots \\ \mathbf{J}_N|^{m+\frac{1}{2}} \end{array} \right]. \tag{18}$$

Similarly, the column vector $\boldsymbol{\eta}|^m$ is built up by arraying the auxiliary electromagnetic field quantities $\boldsymbol{\eta}_k|^m$ $(k = 1,2,\ldots,N)$ as defined in (15). It is worth noting that the inverse of the coefficient matrix $\underline{\mathbf{T}}$ of the linear system (17) can be conveniently computed only one time before the time–marching scheme is initiated. In this way, in comparison to the *FDTD* procedure described in [1], the algorithmic implementation of the technique proposed in this research study actually results in a reduced additional computational cost of $O\left(N^2\right)$ floating–point operations useful to determine the solution of (15) as $\mathbf{J}|^{m+\frac{1}{2}} = \underline{\mathbf{T}}^{-1} \cdot \boldsymbol{\eta}|^m$.

Once the current density terms $\mathbf{J}_l|^{m+\frac{1}{2}}$ $(l = 1,2,\ldots,N)$ are evaluated, the electric field distribution within the considered dielectric medium can be derived from (5) as:

$$\mathbf{E}|^{m+\frac{1}{2}} = \frac{2\varepsilon_0\varepsilon_{r_\infty} - \sigma\Delta t}{2\varepsilon_0\varepsilon_{r_\infty} + \sigma\Delta t}\, \mathbf{E}|^{m-\frac{1}{2}} + \frac{2\Delta t}{2\varepsilon_0\varepsilon_{r_\infty} + \sigma\Delta t} \left[(\nabla \times \mathbf{H})|^m - \frac{1}{2} \sum_{l=1}^{N} \left(\mathbf{J}_l|^{m-\frac{1}{2}} + \mathbf{J}_l|^{m+\frac{1}{2}} \right) \right], \tag{19}$$

where judicious use of (9) has been made. Finally, by carrying out a second–order accurate finite–difference approximation of the Faraday's law in the time domain, the following update equation for the magnetic field is readily obtained:

$$\mathbf{H}|^{m+1} = \mathbf{H}|^m - \frac{\Delta t}{\mu_0} (\nabla \times \mathbf{E})|^{m+\frac{1}{2}}, \tag{20}$$

with μ_0 denoting the magnetic permeability of free space.

C. Numerical Stability

Following the von Neumann's spectral approach for the stability analysis of finite–difference schemes [5], [16], let's assume a harmonic time dependence $e^{j\omega t}$ of the electromagnetic field quantities in the foregoing. At any discrete time step, the instantaneous distributions of $\mathbf{E}$, $\mathbf{H}$, and $\mathbf{J}_l$ vectors for $l = 1,2,\ldots,N$ can be Fourier–transformed with respect to the space variable x to provide a spectrum of monochromatic

plane–wave modes propagating along the computational lattice. By using the usual *FDTD* notation, one can write for the individual eigenmode:

$$\left\{ \begin{array}{c} \mathbf{E} \\ \mathbf{H} \\ \mathbf{J}_l \end{array} \right\}\Bigg|_h^m = \left\{ \begin{array}{c} \widehat{\mathbf{E}} \\ \widehat{\mathbf{H}} \\ \widehat{\mathbf{J}}_l \end{array} \right\} e^{j(\omega m\Delta t - \xi h\Delta x)}, \tag{21}$$

with Δx and ξ being, respectively, the increment step of the grid, and the real wavenumber of the arbitrary harmonic field component. In (21), $\widehat{\mathbf{E}}$, $\widehat{\mathbf{H}}$, $\widehat{\mathbf{J}}_l$ denote the amplitude vectors relevant to the corresponding wave quantities.

Under the mentioned hypotheses, the central finite–difference approximations of the first–order derivatives in time and space degenerate in algebraic multiplication operators which can be expressed in terms of the unnormalized cardinal sine function as follows:

$$\left\{ \begin{array}{l} \partial_t \rightarrow j\Omega(\omega) = j\omega \operatorname{sinc} \frac{\omega\Delta t}{2}, \\ \partial_x \rightarrow -j\Xi(\xi) = -j\xi \operatorname{sinc} \frac{\xi\Delta x}{2}, \end{array} \right. \tag{22}$$

so that the update equations of the electric and magnetic fields at the general nodal point $x = h\Delta x$ and time instant $t = m\Delta t$ become:

$$\left[\begin{array}{cc} \varepsilon_0 \widetilde{\varepsilon}_r(\omega)\Omega(\omega) & \Xi(\xi) \\ \Xi(\xi) & \mu_0\Omega(\omega) \end{array} \right] \cdot \left[\begin{array}{c} \mathbf{E}|_h^m \\ \mathbf{H}|_h^m \end{array} \right] = \left[\begin{array}{c} \mathbf{0} \\ \mathbf{0} \end{array} \right], \tag{23}$$

where:

$$\widetilde{\varepsilon}_r(\omega) = \varepsilon_{r_\infty} + \rho(\omega) \left[\sum_{l=1}^{N} \frac{\Delta\varepsilon_{r_l}}{\gamma_l(j\omega\tau_l)} + \frac{\sigma}{j\Omega(\omega)\varepsilon_0} \right], \tag{24}$$

with $\rho(\omega) = \cos\frac{\omega\Delta t}{2}$ and, assuming that the effect of the initial and boundary conditions can be neglected:

$$\gamma_l(j\omega\tau_l) = \lim_{m\rightarrow+\infty} \frac{\left(\mathscr{D}_t^{(l)}\mathbf{J}_l\right)\Big|_h^m \cdot \left(\mathbf{J}_l|_h^m\right)^*}{\left\|\mathbf{J}_l|_h^m\right\|^2} = \sum_{n=0}^{K_l} \chi_{n,l} \left[j\Omega(\omega)\tau_l\right]^{\nu_{n,l}} \cdot e^{-j\left(\nu_{n,l}-1\right)\frac{\omega\Delta t}{2}} \frac{\left(\Delta t/\tau_l\right)^{\nu_{n,l}-\zeta_{n,l}}}{\left(\nu_{n,l}-\zeta_{n,l}\right)!} \sum_{q=1}^{Q_{n,l}} \frac{a_{n,l,q}}{1-e^{-b_{n,l,q}-j\omega\Delta t}}, \tag{25}$$

where the superscript * denotes the complex conjugation. For brevity, the details of the derivations are not included here since they are quite lengthy, though not complicated.

For the electromagnetic field update equations (23) to admit a non–trivial solution, the relevant determinant must be forced to zero, this leading to the dispersion relation:

$$\Xi^2(\xi) - \left[\frac{\Omega(\omega)}{c_0}\right]^2 \widetilde{\varepsilon}_r(\omega) = 0, \tag{26}$$

c_0 being the speed of light in free space. Upon introducing the numerical amplification factor over time as:

$$z = \exp\left(j\frac{\omega\Delta t}{2}\right), \tag{27}$$

it is not difficult to verify that:

$$\left\{ \begin{array}{c} j\Omega\Delta t \\ 2\rho \end{array} \right\} = \frac{1}{z}\left(z^2 \left\{ \begin{array}{c} - \\ + \end{array} \right\} 1\right). \tag{28}$$

Similarly, the relative permittivity $\widetilde{\varepsilon}_r$ turns into a rational function of z, namely:

$$\widetilde{\varepsilon}_r(z) = \frac{\widetilde{N}_r(z)}{\widetilde{D}_r(z)}. \tag{29}$$

In this way, the characteristic polynomial equation of the proposed *FDTD* algorithm is easily derived from (26) as:

$$\left[c_0\Delta t\,\Xi(\xi)\,z\right]^2 \widetilde{D}_r(z) + \left(z^2-1\right)^2 \widetilde{N}_r(z) = 0, \tag{30}$$

subject to the condition $\widetilde{D}_r(z) \neq 0$.

The eigenvalues z_i $(i = 1, 2, \ldots)$ satisfying (30) can be easily determined by using the Jenkins–Traub root–finding method, which is characterized by global convergence for polynomials with complex–valued coefficients [17]. Clearly, the numerical stability of the proposed time–marching scheme is verified if the following condition on the spectral radius of the polynomial (30):

$$\max_i |z_i| \leqslant 1, \tag{31}$$

holds true for any spatial frequency $\xi \in [0, \pi/\Delta x]$ once a given Courant factor $S = c_0\Delta t/\Delta x \leqslant 1$ is selected.

D. Uniaxial Perfectly Matched Layer Boundary Conditions

In order to truncate the *FDTD* computational domain and solve electromagnetic problems with open boundaries, dedicated uniaxial perfectly matched layer (*UPML*) conditions [18] have to be derived and implemented numerically accounting for the electrical conductivity and the multi–relaxation characteristics of the dielectric material under analysis. To this end, let us first introduce the auxiliary electric field vector $\mathbf{e}$ as:

$$\mathbf{e} = \left(\kappa_x + \frac{\sigma_x}{j\omega\varepsilon_0}\right)\mathbf{E}, \tag{32}$$

with κ_x, σ_x denoting the *UPML* material parameters in accordance with the complex coordinate stretching approach [5]. Multiplying both sides of (32) by $j\omega$ and transforming into the time domain immediately yields:

$$\partial_t\mathbf{e} = \kappa_x\partial_t\mathbf{E} + \frac{\sigma_x}{\varepsilon_0}\mathbf{E}. \tag{33}$$

In this way, it is not difficult to find out that the Ampere's law can be written, within the *UPML* region, as:

$$\nabla\times\mathbf{H} = \varepsilon_0\varepsilon_{r_\infty}\partial_t\mathbf{e} + \sigma\mathbf{e} + \sum_{l=1}^{N}\mathbf{j}_l, \tag{34}$$

where the $l-$th displacement current density term $(1 \leq l \leq N)$ satisfies the fractional derivative equation:

$$\mathscr{D}_t^{(l)}\mathbf{j}_l = \varepsilon_0\Delta\varepsilon_{r_l}\partial_t\mathbf{e}. \tag{35}$$

The discretization of the considered equations on the Yee lattice can be conveniently carried out by adopting the usual leapfrog scheme in time, wherein the loss terms are averaged according to the semi–implicit approximation [see (9)]. Overall, as it can be easily figured out by comparison with (5) and (6), this leads to time–stepping expressions which are formally equivalent to (15) and (19) with the stretched vectors $\mathbf{e}$ and $\mathbf{j}_l$ replacing the quantities $\mathbf{E}$ and $\mathbf{J}_l$, respectively, for

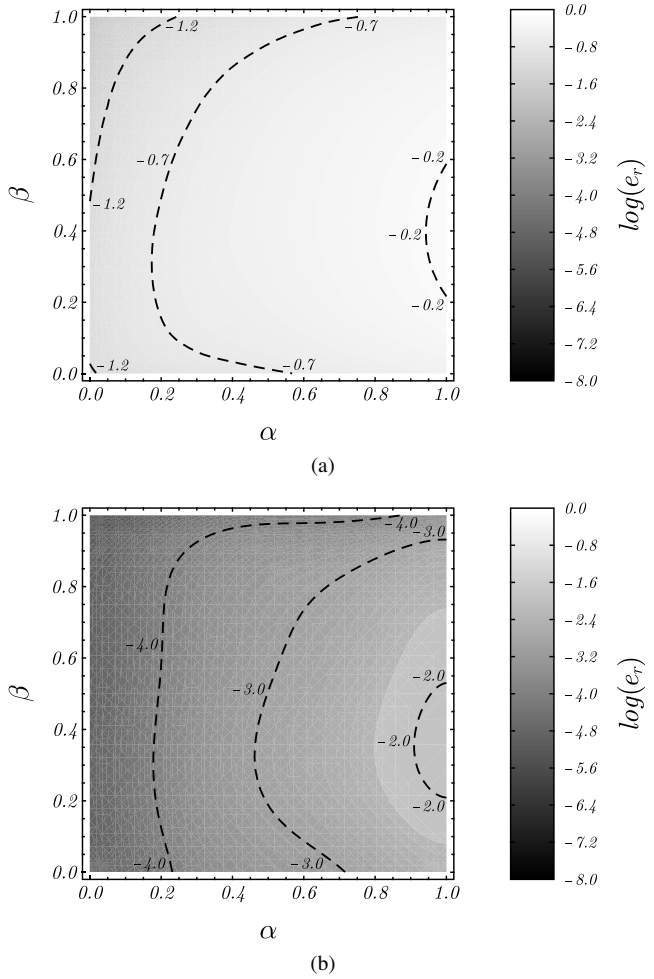

Fig. 1. Distribution of the relative error e_r as a function of the model parameters α and β relevant to a *HN* dielectric material with single relaxation time $\tau = 140$ ps as computed by (*a*) the procedure detailed in [1] and (*b*) the methodology developed in this study. The normalized working frequency range is $0.1 \leqslant \omega\tau \leqslant 10$.

$l = 1, 2, \ldots, N$. On the other hand, the electric field update equation directly follows from (33) as:

$$\mathbf{E}\big|^{m+\frac{1}{2}} = \frac{2\varepsilon_0\kappa_x - \sigma_x\Delta t}{2\varepsilon_0\kappa_x + \sigma_x\Delta t}\,\mathbf{E}\big|^{m-\frac{1}{2}} + \frac{2\varepsilon_0}{2\varepsilon_0\kappa_x + \sigma_x\Delta t} \cdot \left(\mathbf{e}\big|^{m+\frac{1}{2}} - \mathbf{e}\big|^{m+\frac{1}{2}}\right). \tag{36}$$

Finally, by Fourier–transforming the Faraday's law $\nabla\times\mathbf{E} = -\mu_0\,(j\omega\kappa_x + \sigma_x/\varepsilon_0)\,\mathbf{H}$ and discretizing at the time instance $t = \left(m+\frac{1}{2}\right)\Delta t$, one can readily derive the time–stepping expression for the magnetic field within the *UPML* termination:

$$\mathbf{H}\big|^{m+1} = \frac{2\varepsilon_0\kappa_x - \sigma_x\Delta t}{2\varepsilon_0\kappa_x + \sigma_x\Delta t}\,\mathbf{H}\big|^{m} - \frac{2Y_0^2\Delta t}{2\varepsilon_0\kappa_x + \sigma_x\Delta t}\,(\nabla\times\mathbf{E})\big|^{m+\frac{1}{2}}, \tag{37}$$

with $Y_0 = \sqrt{\varepsilon_0/\mu_0}$ being the wave admittance in free space.

III. Numerical Results

The validation of the developed numerical procedure has been carried out by different one–dimensional test cases involving complex dispersive dielectric materials under plane–wave excitation. To this end, the conventional total field/scattered field (*TF/SF*) formulation detailed in [5] has been implemented using a sinusoidally time–modulated Gaussian pulse source polarized along the y axis:

$$\mathbf{I}_s(x,t) = \exp\left[-\left(\frac{t-T_c}{T_d}\right)^2\right]\sin\left[2\pi f_e\,(t-T_c)\right]\delta(x-x_s)\,\hat{\mathbf{y}}, \tag{38}$$

with $\delta(\cdot)$ denoting the usual Dirac delta distribution, and where the parameters $T_d = 0.475/f_e$, $T_c = 4T_d$, $f_e = 6$ GHz have been selected in such a way as to achieve a spectral bandwidth of about 10 GHz.

In all computations, the truncates series representation of the fractional derivative operators related to the considered dispersive materials is derived by means of the *EWQPSO*–based fitting algorithm described in the previous section, while enforcing the passivity of the approximated permittivity function in order to ensure the physical consistency of the model. In doing so, the error threshold $\delta = 10^{-6}$ and expansion order $K = 5$ have been adopted.

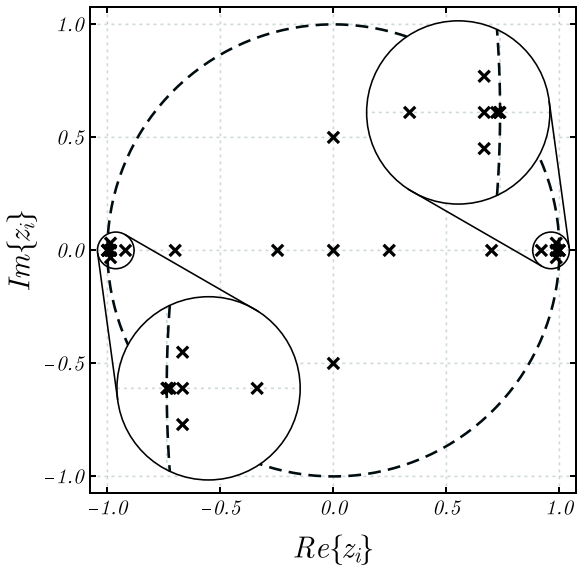

Fig. 2. Location of the zeros z_i of the stability polynomial associated with the *FDTD* scheme used to characterize a *HN* dielectric material with parameters $\alpha = 0.9$, $\beta = 0.3$, $\varepsilon_{r_\infty} = 4$, $\Delta\varepsilon_r = 88$, $\sigma = 0$ S/m, and $\tau = 140$ ps, under the assumption of a Courant factor $S = 1$, and normalized spatial frequency $\xi\Delta x = \pi$. The unit circle is also shown.

A. Single–Layered HN Dielectric Slab

The first test case is relevant to a single–layered *HN* dielectric slab in air. The material parameters are $\alpha = 0.9$, $\beta = 0.3$, $\varepsilon_{r_\infty} = 4$, $\Delta\varepsilon_r = 88$, $\sigma = 0$ S/m, and $\tau = 140$ ps, the thickness of the slab being $d = 10$ mm.

Fig. 1 shows, in logarithmic scale, the relative fitting error e_r associated with the expansion (3) as a function of α and β, in comparison to the one achieved by means of the truncated binomial series approximation illustrated in [1]. As it can be noticed, the newly introduced methodology provides a significantly larger accuracy in the representation of the *HN* fractional derivative operator with a maximum error value, over the complete problem space, of about 4.2% contrary to

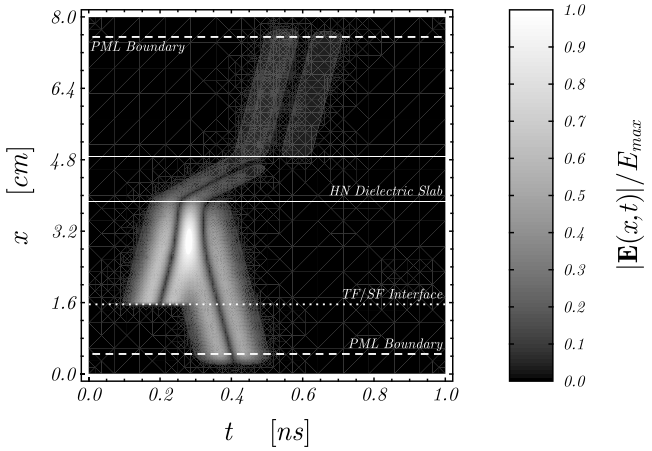

Fig. 3. Normalized space–time distribution of the electric field resulting from the plane–wave excitation of a single–layered *HN* dielectric slab located in air, as computed by the proposed *FDTD*–based procedure.

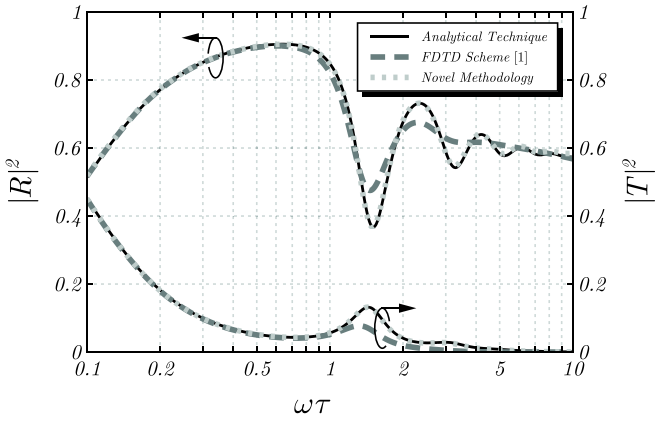

Fig. 4. Reflectance and transmittance versus frequency of a *HN* dielectric slab with dispersion parameters $\alpha = 0.9$, $\beta = 0.3$, and single relaxation time $\tau = 140$ ps. The thickness of the slab is $d = 10$ mm.

the methodology in [1] which, on the other hand, can result in a maximal error of about 45.0%, this being due to the fact that, for the selected *HN* parameters, the truncated binomial series, even if it is never divergent, provides a poor approximation accuracy for $\omega\tau > 1$.

In order to check the numerical stability of the proposed algorithm based on the derived optimal fractional expansion with terms $(\zeta_0 = 0,\ \chi_0 = 1)$, $(\zeta_1 = 0.6428,\ \chi_1 = 0.2591)$, $(\zeta_2 = 0.0249,\ \chi_2 = 1.0942 \times 10^{-16})$, $(\zeta_3 = 9.766 \times 10^{-7},\ \chi_3 = 1.4302 \times 10^{-18})$, $(\zeta_4 = 5.8399 \times 10^{-8},\ \chi_4 = 5.6964 \times 10^{-20})$, $(\zeta_5 = 1.0758 \times 10^{-7},\ \chi_5 = 4.2302 \times 10^{-20})$, the von Neumann's spectral criterion detailed in the previous section has been applied. To this end, the location of the zeros z_i $(i = 1, 2, \ldots)$ of the characteristic equation (30) has been analyzed as a function of the Courant factor S, and the normalized spatial frequency $\xi\Delta x$ of the general plane–wave mode propagating within the *FDTD* lattice. In this way, it has been found out that the spectral radius $\max_i |z_i|$ of the polynomial (30) is always smaller than unity. In particular, the characteristic zeros tend to get closer to the unit circle as $S \to 1$ and $\xi\Delta x \to \pi$, when the relevant distribution is as shown in Fig. 2.

TABLE I
CHARACTERISTICS OF A THREE–LAYERED *HN* DIELECTRIC SLAB WITH SINGLE RELAXATION TIME.

medium	α	β	τ (ps)	$\Delta\varepsilon_r$	σ (S/m)	$\varepsilon_{r\infty}$	d (mm)
1	0.85	0.3	135	48	0	4	10
2	0.9	0.5	155	65	0.01	2.5	5
3	0.8	0.8	140	33	0.06	2.5	15

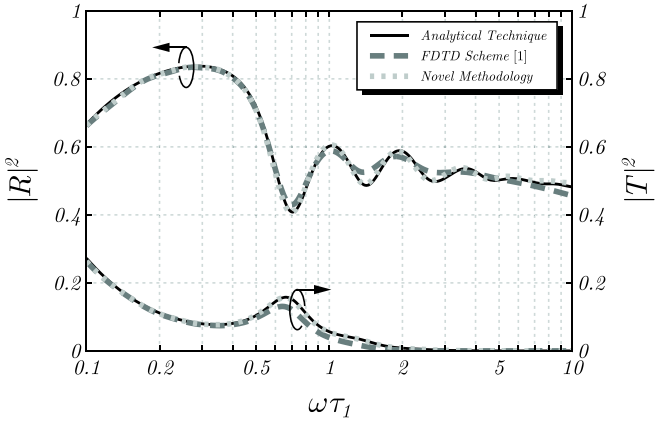

Fig. 5. Reflectance and transmittance versus frequency of a three–layered *HN* dielectric slab with single relaxation time (see Table I).

Fig. 3 shows the space–time distribution of the electric field resulting from the plane–wave illumination of the considered *HN* dielectric slab, as computed by means of the developed *FDTD* procedure. The wave contributions associated with the reflection and transmission processes can be easily identified by visual inspection. Starting from the space–time field distribution, the frequency–domain behavior of reflectance and transmittance of the slab has been evaluated, and compared to the same quantities determined by using the methodology in [1], as well as a rigorous fully analytical technique based on the transfer matrix approach for the characterization of layered lossy media in frequency domain. The excellent agreement with the analytical technique validates the proposed methodology. On the other hand, the inappropriateness of the original *FDTD* scheme [1] to model the considered *HN* medium at high frequencies is apparent.

B. Multi–Layered HN Dielectric Slab

The second test case consists of a three–layered *HN* dielectric slab in air, featuring the geometrical and electrical parameters listed in Table I. As it can be observed in Fig. 5, even in this case, the new *FDTD* formulation allows a more accurate electromagnetic modeling in comparison to the original scheme in [1], the difference being more noticeable at higher frequencies.

The third test case is the more general one since it is relevant to the electromagnetic characterization of a three–layered dispersive dielectric slab over an ultra–wide frequency band spanning from $f_{\min} = 100$ MHz to $f_{\max} = 10$ GHz. Each layer of the slab is assumed to be made out of a *HN* medium

TABLE II
CHARACTERISTICS OF A THREE–LAYERED *HN* DIELECTRIC SLAB WITH MULTIPLE RELAXATION TIMES.

medium	$\alpha_{1,2}$	$\beta_{1,2}$	$\tau_{1,2}$ (ns)	$\Delta\varepsilon_{r_{1,2}}$	σ (S/m)	ε_{r_∞}	d (mm)
1	0.93	0.5	0.008	37	0	4	8
	0.92	0.57	6.8	179			
2	0.92	0.6	0.0083	2.3	0.01	2.5	10
	0.91	0.35	2.3	79.2			
3	0.91	0.7	0.0138	8.2	0.06	2.5	12
	0.7	0.3	6.4	130			

TABLE III
CHARACTERISTICS OF A THREE–LAYERED *R* DIELECTRIC SLAB WITH MULTIPLE RELAXATION TIMES.

medium	$\alpha_{1,2}$	$\beta_{1,2}$	$s_{1,2}$	$\tau_{1,2}$ (ns)	$\Delta\varepsilon_{r_{1,2}}$	σ (S/m)	ε_{r_∞}	d (mm)
1	0.8	0.7	0.9	0.008	2	0	4	5
	0.7	0.8	0.1	7	33			
2	0.8	0.2	0.1	0.016	3	0.01	2.5	10
	0.2	0.85	0.75	0.2	80			
3	0.2	0.8	0.9	0.005	50	0.07	2	6
	0.8	0.6	0.8	0.06	6			

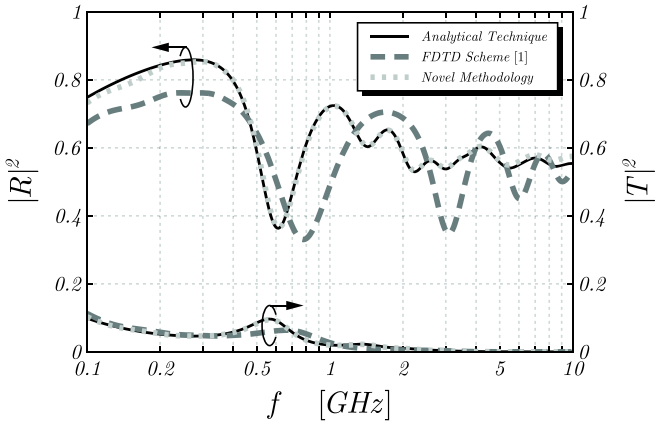

Fig. 6. Reflectance and transmittance versus frequency of a three–layered *HN* dielectric slab with multiple relaxation times (see Table II).

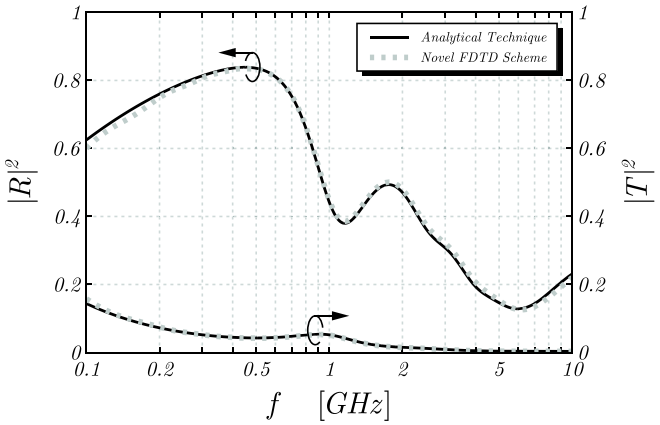

Fig. 7. Reflectance and transmittance versus frequency of a three–layered *R* dielectric slab with multiple relaxation times (see Table III).

having the geometrical and electrical parameters listed in Table II. In order to assess the reliability and robustness of the developed numerical code, very different relaxation times $\tau_{i,j}$ are considered across the various material layers. As a matter of fact, with the specific choice of parameters in Table II, the normalized frequency $2\pi f_{\max}\tau_{i,j}$ ranges from about 0.5 to about 430. The frequency–domain behavior of the slab reflectance and transmittance evaluated by means of the proposed *FDTD* procedure, as well as the scheme in [1], and the aforementioned analytical transfer–matrix–based approach, is reported in Fig. 6. It is apparent from the obtained results that the original *FDTD* technique in [1] is not suitable for handling complex material dispersion characteristics.

Further numerical investigations have shown that the conventional binomial series approximation introduced in [1] to characterize *HN* materials becomes inaccurate when the normalized frequency $\omega\tau$ is larger than 10 as, on the other hand, it typically occurs in biological media displaying complex dispersion mechanisms. Conversely, the methodology illustrated in Section II tends to be, always, in excellent agreement with theory over ultra–broad frequency ranges.

C. Multi–Layered R Dielectric Slab

The Raicu dispersion function has been recently introduced in the scientific literature in order to enable an accurate description of the dielectric properties of a wide range of biological tissues in close agreement with experimental data [19]. This model, resulting from the generalization of Debye–like (*D*, *CC*, *CD*, *HN*) and Jonscher's universal responses, can actually describe the classical relaxation mechanisms in combination with the effect of the interfacial polarization across cell membranes.

The *R* equation includes all the classical dispersion functions as its special cases. However, the complexity associated with the higher–order fractional–power–law structure of the representation poses non–trivial problems in the embedding of the model, as such, into the core of an existing *FDTD* scheme. Said drawback can be, however, overcome easily by making use of the proposed methodology.

As a matter of fact, the final test case pertains the electromagnetic analysis, in the frequency band between $f_{\min} = 100$ MHz and $f_{\max} = 10$ GHz, of a three–layered *R* dielectric slab located in air, and featuring the geometrical and electrical characteristics listed in Table III. In this case, the developed *FDTD* algorithm is even more stressed in comparison to the previously considered examples, since the normalized frequency $2\pi f_{\max}\tau_{i,j}$ spans three decades ranging from about 0.3 to about 440. Fig. 7 shows the reflectance and transmittance versus frequency as calculated by means of the developed time–domain technique and the analytical transfer–matrix–based method in frequency domain. Clearly, the agreement between the two approaches is very good. Here, no comparison with the *FDTD* formulation illustrated in [1] is possible since that procedure is not applicable to the study of electromagnetic wave propagation in *R* dielectric materials.

IV. CONCLUSION

A novel *FDTD* technique based on the fractional derivative

operator theory has been presented. The developed numerical approach allows analyzing short–pulse wave propagation in general layered dispersive materials characterized by multiple relaxation times, while overcoming some drawbacks limiting the applicability of the fractional–calculus–based approach previously published by the authors at high frequencies. Dedicated *UPML* boundary conditions have been derived and implemented in combination with the basic time–marching scheme. Furthermore, the numerical stability of the proposed procedure has been analyzed by means of the von Neumann's spectral approach, and the relevant numerical dispersion equation has, also, been derived.

The soundness and reliability of the modified *FDTD* procedure has been assessed by several test cases involving dielectrics featuring, among others, *HN* and *R* dispersion characteristics. The obtained results show a good agreement with theory, and confirm the enhancement of the numerical accuracy of the new methodology in comparison with the previously introduced one, especially when the ultra–wideband characterization of multi–relaxed media is to be carried out.

The presented technique provides a general–purpose tool useful to address complex electromagnetic problems in the field of bio–engineering. Its application to the study of temperature elevation in biological tissues subject to *PEF* excitation, as well as the investigation of electroporation processes in cells exposed to high–voltage electric pulses is currently ongoing.

REFERENCES

[1] L. Mescia, P. Bia, and D. Caratelli, "Fractional derivative based FDTD modeling of transient wave propagation in Havriliak–Negami media," *IEEE Trans. Microw. Theory Tech.*, vol. 62, pp. 1920–1929, 2014.

[2] P. Bia, D. Caratelli, L. Mescia, R. Cicchetti, G. Maione, and F. Prudenzano, "A novel FDTD formulation based on fractional derivatives for dispersive Havriliak–Negami media," *Signal Processing*, vol. 107, pp. 312–318, 2015.

[3] A. A. Khamzin, R. R. Nigmatullin, and I. I. Popov, "Log–periodic corrections to the Cole–Cole expression in dielectric relaxation," *Physica A*, vol. 392, pp. 136–148, 2013.

[4] K. Foster and H. Schwan, "Dielectric properties of tissues," *Biological Effects of Electromagnetic Fields*, C. Polk and E. Postow, Eds. New York, NY, USA: CRC Press, 1996.

[5] A. Taflove and S. Hagness, *Computational Electrodynamics: The Finite–Difference Time–Domain Method*. Norwood, MA, USA: Artech House, 2005.

[6] D. Caratelli, A. Massaro, R. Cingolani, and A. Yarovoy, "Accurate time–domain modeling of reconfigurable antenna sensors for non–invasive melanoma skin cancer detection," *IEEE Sensors J.*, vol. 12, pp. 635–643, 2012.

[7] W. J. Chen, W. Shao, and B. Z. Wang, "ADE–Laguerre–FDTD method for wave propagation in general dispersive materials," *IEEE Microw. Wireless Compon. Lett.*, vol. 23, pp. 228–230, 2013.

[8] M. F. Causley and P. G. Petropoulos, "On the time–domain response of Havriliak–Negami dielectrics," *IEEE Trans. Antennas Propag.*, vol. 61, pp. 3182–3189, 2013.

[9] S. G. Ha, J. Cho, H. Kim, and K. Y. Jung, "FDTD Dispersive Modeling of Human Tissues Based on Quadratic Complex Rational Function,"*IEEE Trans. Antennas Propag.*, vol. 61, pp. 996–999, 2013.

[10] L. Mescia, P. Bia, and D. Caratelli, "Authors reply," *IEEE Trans. Microw. Theory Tech.*, vol. 63, pp. 4191–4193, 2015.

[11] Y. Feldman, A. Puzenko, and Y. Ryabov, "Dielectric relaxation phenomena in complex materials," *Fractals, Diffusion, and Relaxation in Disordered Complex Systems: Advances in Chemical Physics*, W. T. Coffey and Y. P. Kalmykov, Eds., Part A, vol. 133. Hoboken, NJ, USA: John Wiley & Sons, 2006.

[12] P. Bia, D. Caratelli, L. Mescia, and J. Gielis, "Analysis and synthesis of supershaped dielectric lens antennas," *IET Microw. Antennas Propag.*, doi: 10.1049/iet–map.2015.0091, 2015.

[13] M. Avriel, *Nonlinear Programming: Analysis and Methods*. Englewood Cliffs, NJ: Prentice–Hall, 1976.

[14] D. Ashlock, *Evolutionary Computation for Modeling and Optimization*. New York, NY: Springer, 2005.

[15] A. Giaquinto, L. Mescia, G. Fornarelli, and F. Prudenzano, "Particle swarm optimization–based approach for accurate evaluation of upconversion parameters in Er^{3+}–doped fibers," *Opt. Lett.*, vol. 36, pp. 142–144, 2011.

[16] J. A. Pereda, L. A. Vielva, A. Vegas, and A. Prieto, "Analyzing the stability of the FDTD technique by combining the von Neumann method with the Routh-Hurwitz criterion," *IEEE Trans. Microw. Theory Tech.*, vol. 49, pp. 377-381, 2001.

[17] M. A. Jenkins and J. F. Traub, "A three–stage variables–shift iteration for polynomial zeros and its relation to generalized Rayleigh iteration," *Numer. Math.*, vol. 14, pp. 252–263, 1970.

[18] S. D. Gedney, "An anisotropic perfectly matched layer absorbing medium for the truncation of FDTD lattices," *IEEE Trans. Antennas Propagat.*, vol. 44, pp. 1630-1639, 1996.

[19] V. Raicu, "Dielectric dispersion of biological matter: model combining Debye–type and universal responses," *Phys. Rev. E*, vol. 60, pp. 4677–4680, 1999.

Diego Caratelli was born in Latina, Italy on May 2, 1975. He received the Laurea (summa cum laude) and Ph.D. degrees in Electronic Engineering, as well the M.Sc. degree (summa cum laude) in Applied Mathematics from Sapienza University of Rome, Italy in 2000, 2004, and 2013, respectively. He has been Research Fellow at the Department of Electronic Engineering, Sapienza University of Rome, from 2005 to 2007, and Senior Researcher at the International Research Centre for Telecommunications and Radar of Delft University of Technology, the Netherlands, from 2007 to 2013. In 2013 he has co–founded The Antenna Company, where is currently Chief Technology Officer. He is, also, Associate Professor at the Institute of Cybernetics of Tomsk Polytechnic University, Russia, since 2014, as well as Visiting Researcher in the group of Electromagnetics in Wireless Telecommunications at Eindhoven University of Technology, the Netherlands, since 2015.

His main research interests include the full–wave analysis and design of passive devices and antennas for satellite, wireless and radar applications, the development of analytically–based numerical techniques devoted to the modeling of wave propagation and diffraction processes, as well as the theory of special functions for electromagnetics, the deterministic synthesis of sparse antenna arrays, and the solution of boundary–value problems for partial differential equations of mathematical physics. His research activity has so far resulted in more than one hundred publications in international journals, book chapters, and conference proceedings.

Dr. Caratelli was the recipient of the Young Antenna Engineer Prize at the 32th European Space Agency Antenna Workshop. He received the 2010 Best Paper Award from the Applied Computational Electromagnetics Society (*ACES*). He is a member of *ACES*, and the Italian Electromagnetic Society (*SIEm*).

Luciano Mescia received the Master degree in electronic engineering in 2000, and the Ph.D. degree in electromagnetic fields in 2003.

In January 2005, he joined the Politecnico of Bari, Bari, Italy, as an Assistant Professor, and became Associate Professor in October 2015. His research interests include the development of artificial neural networks, genetic algorithms, and swarm intelligence applied to rare earth doped fiber lasers and amplifiers. He performs studies regarding the design of innovative antennas for energy harvesting applications, the analysis and synthesis of novel dielectric lens antennas operating in the microwave and millimeter frequency range, and the development of novel *FDTD* schemes based on fractional calculus. He has cooperated with many national and international research institutions and he joined several research projects with academic and industrial partners. His research has resulted in over 100 publications in high–impact *ISI* scientific and engineering peer–reviewed journals, leading international conferences, lectures, and invited papers.

Prof. Mescia is a member of the Italian Society of Optics and Photonics (*SIOF*) and the Italian Society of Electromagnetism (*SIEm*).

Pietro Bia received the Master degree in electronic engineering in 2010, and the Ph.D. degree in electromagnetic fields in 2015, both from Politecnico of Bari, Bari, Italy.

In 2011, he attended a Master second–level course on "Technologies for space remote sensing" at Politecnico of Bari. His research is focused on the analysis of dielectric lens antennas for microwave application and *FDTD* modeling for *PEF* propagation in complex dispersive media.

Dr. Bia is a member of the Italian Society of Optics and Photonics (*SIOF*) and the Italian Society of Electromagnetism (*SIEm*). He was the recipient of the Best Italian Geoscience and Remote Sensing Thesis Prize of the *IEEE GRSS* Italian Chapter in 2008. In 2011 he received a scholarship for post–graduate research activities for the topic: "Design of innovative cladding–pumped fiber lasers, nonlinear effects induced by high optical power density and microsphere laser", and the *IEEE MTT–S* Central–Southern Italy award in 2014 with Honorable Mention for the scientific paper L. Mescia, P. Bia, and D. Caratelli, "Fractional derivative based FDTD modeling of transient wave propagation in Havriliak–Negami media," *IEEE Trans. Microw. Theory Tech.*, vol. 62, pp. 1920–1929, 2014.

Oleg V. Stukach received the Diploma degree in radio engineering (with honors) in 1988 and the Doctor of Technical Sciences degree in modeling, numerical methods, and software in 2010 from Tomsk State University of Control Systems and Radioelectronics, Tomsk, Russia.

In 1988, he joined the Picosecond Technique Labs, Tomsk, Russia. Currently, he is Professor, Chair of department of Computer-Aided Measurement Systems and Metrology of the Tomsk Polytechnic University, Russia. He has published more than 200 technical papers and patents in the fields of microwave technique, *GPR*, and theory of control. His principal area of specialization includes theory of parametric invariance of the nonlinear systems.

Since 1995, Dr. O. Stukach serves as Chair of the biennal International Siberian Conference on Control and Communications SIBCON. He is organizer and active participant of international scientific conferences, winner of the Tomsk Region Prize in science and education.